Cellular Physiology and Biochemistry

Cell Physiol Biochem 2013;31:614-624
DOI: 10.1159/000350081
Published online: May 06, 2013
Accepted: April 18, 2013

1421-9778/13/0315-0614$38.00/0

Original Paper

Intracerebral Administration of Heat-Inactivated *Staphylococcus Epidermidis* Enhances Oncolysis and Prolongs Survival in a 9L Orthotopic Gliosarcoma Model

Mario Löhr[a,f] Marek Molcanyi[a,e] Jörg Poggenborg[b] Elmar Spuentrup[b] Matthias Runge[c] Gabriele Röhn[a] Wolfgang Härtig[d] Jürgen Hescheler[e] Jürgen A. Hampl[a]

[a]Neurosurgical Oncology Laboratory, Department of General Neurosurgery, University Hospital Cologne, Cologne, [b]Department of Radiology, University Hospital Cologne, Cologne, [c]Department of Stereotactic and Functional Neurosurgery, University Hospital Cologne, Cologne, [d]Paul Flechsig Institute for Brain Research, University of Leipzig, Leipzig, [e]Center of Physiology, Institute of Neurophysiology, Medical Faculty, University of Cologne, Cologne; [f]Department of Neurosurgery, University of Wuerzburg, Wuerzburg

Key Words
Glioblastoma • Immunotherapy • Oncolysis • *Staphylococcus* • Immunostimulatory adjuvant

Abstract
Background/Aims: The association between postoperative infection and prolonged survival in high-grade glioma is still a matter of debate. Previously we demonstrated that the intracerebral (i.c.) injection of heat-inactivated staphylococcal epitopes (HISE) resulted in a well-defined influx of immunocompetent cells across the blood-brain barrier. The present study investigated the potential antitumoral effect of HISE-immunostimulation in an experimental glioma model. ***Methods:*** Wistar rats were intracerebrally implanted with 9L gliosarcoma cells (n=6), 9L cells mixed with HISE (n=12), or phosphate buffered saline (n=4). Tumor growth was measured by serial magnetic resonance imaging (MRI). After death due to the tumor burden, the brains were histopathologically assessed for inflammation and oncolysis. A toxicity assay was performed to quantify potential impairment of HISE on tumor cell growth *in vitro*. ***Results:*** Animals treated by HISE showed a significant increase in average survival and even complete regression of an already established mass in one case. Naïve 9L gliosarcomas failed to recruit significant numbers of systemic immune cells. In contrast, concomitant intracerebral HISE inoculation lead to a oncolysis and a distinct peri- and intratumoral infiltration of macrophages, CD8 and CD4 co-expressing T-lymphocytes in two thirds of the tumor-bearing animals. The toxicity screening showed HISE-mediated oncolysis to be ineffective *ex vivo*. ***Conclusion:*** This study describes a novel approach for combatting malignant glioma using inactivated staphylococci as potent immunomodulators. Our results provide an outline for investigating the strategic potential of bacteria as emerging future therapeutics.

Mario Löhr, M.D.
Department of Neurosurgery University of Wuerzburg,
Josef-Schneider-Strasse 11, 97080 Wuerzburg (Germany)
Tel. +49-931-201 24807, Fax +49-931-201 624805
E-Mail loehr.m@nch.uni-wuerzburg.de

Introduction

Despite advances in surgical techniques, radio- and chemotherapy, the outcome of patients suffering from glioblastoma multifomre (GBM) remains poor with a median survival of less than 15 months [1]. Whereas the diffuse infiltration of malignant gliomas considerably limits the results of surgical treatment and irradiation, the success of chemo- or receptor-based therapies are restricted by the heterogeneity of glioblastoma surface antigens. Considering the limited effects of current standard treatments, immunotherapeutic strategies are appealing, since stimulated immune effector cells may attack even tumor cells located in areas inaccessible to surgery, chemo- or radiation therapy [2-4].

However, without therapeutic reinforcement, the host´s glioma-directed immune response is hardly effective for several reasons. One reason for the almost exclusive growth of malignant gliomas within the central nervous system (CNS) is their segregation from the systemic immunosurveillance beyond the blood-brain barrier in early tumor growth. Furthermore, GBM escape from an immunogenic response by the release of immunosuppressive cytokines [5, 6], downregulation of MHC class I molecules [7], activating Fas-mediated apoptosis of T-cells [8] and other mechanisms. Therefore, different immunological treatments have been designed to enhance the intrinsic antitumor response that include antibodies targeting tumor-specific antigens [9], vaccination with dendritic cells (DC) [9], adoptive transfer of *ex vivo* activated immune cells with cytolytic properties [10] or boosting endogenous cell-mediated immunity by immunostimulatory adjuvants (ISA) [2].

The latter immunotherapeutic approach is supported by the clinical observation, that postoperative infections within or near the tumor site might have promoted a prolonged survival or even complete remission in several GBM patients [11-15]. Recently these anecdotal findings were substantiated by the results of two retrospective single-center studies, one demonstrating a significant correlation between postoperative infection and survival advantage [16] and the other showing a trend towards a prolonged survival in patients harboring infections in the tumor resection bed in contrast to those with superficial infections [17]. The only study systematically investigating the therapeutic potential of living bacteria to enhance antitumor immunity in GBM reported disastrous effects. By intracarotid injection of spores from the nonpathogenic germ *Clostridium butyricum* in GBM-patients, the malignant mass converted into a putrid abscess within one week that was then operated on. However, one third of the patients died due to a fulminant brain abscess formation caused by a rapid and uncontrollable growth of the bacterial agents [18].

Recently we have demonstrated that the proliferative capacity of *Staphylococcus (S.) epidermidis* and other bacteria could be effectively eliminated by heat-inactivation while maintaining its immunostimulatory properties. Intracerebral (i.c.) injection of inactivated staphylococci into Wistar rats caused a rapid and sustained influx of various systemic immunocompetent cells into the CNS in a reproducible timecourse including, among others, macrophages and $CD8^+$ cytotoxic T-lymphocytes. Moreover, the inflammation was locally restricted to the site of the deposit of the inactivated bacteria, and all experimental animals tolerated the procedure well without signs of cerebral infection [19].

Based on these findings, the specific aim of our study was to investigate if such a distinct intracerebral immune cell recruitment induced by inactivated staphylococci could affect tumor growth in an experimental gliosarcoma model and to shed light on the potential mechanisms by which systemic leucocytes combat malignant glioma.

Materials and Methods

All animal experiments in this study were conducted according to the German law for the welfare of animals and approved by the regional committee on animal ethics (Landesamt für Natur, Umwelt- und Verbraucherschutz Nordrhein-Westfalen, file reference of ethical vote: 9.93.2.10.31.07.305).

Cultivation and inactivation of bacteria

S. epidermidis (strain RP62A) were cultivated in soybean-casein digest broth (Trypticase™ Soy Broth, Becton Dickinson, Heidelberg, Germany) at 37°C for 16 h on a rotary shaker (Bühler™ Shakers, Hechingen, Germany) and concentrated up to 10^{10} colony forming units (cfu)/ml in phosphate buffered saline (PBS). The concentration was determined by counting in a Neubauer-chamber and confirmed by serial plating. Next, bacteria were inactivated at 65°C for 1 h in a water bath. Both inactivation of the bacteria and sterility of the working conditions were verified by plating the stock solution of the heat-inactivated bacteria prior to and after taking out the volumes required for the subsequent experiments.

Tumor cell culture

The 9L gliosarcoma cell line was maintained in Dulbecco´s modified Eagle medium (DMEM) High Glucose supplemented with 5% fetal calf serum Gold (FCS) (PAA Laboratories, Cölbe, Germany) and penicillin-streptavidin in a humidified atmosphere of 5% carbon dioxide at 37°C. The cells were grown to confluence and harvested with trypsin. Cell viability before implantation was estimated by a Trypan blue exclusion test. After determination of the exact concentration by counting in a Neubauer-chamber, the 9L cells were washed twice in endotoxin-free PBS and then adjusted to the concentration required for the following experiments.

In vitro toxicity screening

The 9L cell lines were plated at a density of 10^5 cells/ml in DMEM. Three dishes of heat-inactivated *S. epidermidis* (HISE) were plated for each concentration and three further dishes used as controls. The 9L cells were grown for 24 hours. Thereafter, the medium was removed and replaced by medium containing the concentrations 10^5/ml or $6x10^7$/ml or $6x10^9$/ml of HISE particles, respectively, hence outnumbering the HISE to 9L-ratio of 1:1 used in the injection experiments hundred- to ten-thousand-fold. Pure medium instead of HISE was used in controls. The dishes were incubated for another 5 days, and cells were counted to estimate any impairment of tumor cell growth by HISE *in vitro*.

Animal preparation and operative procedures

All experimental animal protocols were performed under sterile conditions using a laminar air flow bench. For the i.c. injection, HISE and 9L cells were mixed to a concentration of $4x10^6$ HISE particles and $4x10^6$ 9L cells per ml in PBS. Control animals received an equal concentration of only 9L cells in PBS, or pure PBS. 22 male Wistar rats (in-house breeding of the University of Cologne) weighing 350-450g were anesthetized by intraperitoneal injection of ketamine hydrochloride (Ketavet™, Pfizer Co., Karlsruhe, Germany) and xylazine hydrochloride (Rompun™, Bayer Vital Co., Leverkusen, Germany), and placed in a stereotactic frame (Stoelting-Instruments, Wood Dale, IL, USA). After midline incision of the scalp, a 0.006 inch burr hole was placed on the right calvaria 1 mm anterior and 3 mm lateral to the bregma, and a volume of 25 µl of the respective stock solution was administered 6 mm deep into the right striatum by means of convection-enhanced delivery using a programmable syringe pump (Harvard apparatus™ PHD 22/2000, Holliston, MA, USA) at an injection velocity of 1 µl/min. After injection, the needle was kept in place for 5 min to minimize backflow and eventually withdrawn at a rate of 1 mm/min thereafter. Finally, the burr hole was sealed with bone wax, and the skin closed with sutures. Following surgery, the animals were kept under a 12h dark/light-cycle with free access to food and water and were monitored daily for alertness, signs of discomfort or the presence of neurological abnormalities. Altogether n=12 animals received 10^5 9L cells mixed with 10^5 HISE particles in 25 µl of PBS (HISE-group), n=6 received 10^5 9L cells in 25µl of PBS (9L-group), and n=4 received 25 µl of PBS.

MR imaging and tumor volumetry

Magnetic resonance (MR) images were obtained with a clinical scanner (Philips Achieva 1.5 t, Philips Healthcare, Best, The Netherlands) using a 2.3 cm micro ring-coil on days 13 / 19 / 25 / 32 / 40 and 61 post injection (p.i.). 250 µm MR slices were obtained in the following sequence: coronal and sagittal noncontrast T1-weighted images, T2-weighted images, and T1-weighted images 20 minutes after intraperitoneal administration of 1 ml Omniscan™ 0.5 mmol/ml (GE Healthcare Buchler, Braunschweig, Germany), a gadolinium-based contrast agent. Tumor volumes were calculated on the basis of the T1-weighted images with contrast media by using the stereotactic treatment planning software STP* 3.5 (Stryker-Leibinger, Freiburg, Germany).

Tissue preparation

The tumor-bearing animals died either spontaneously or were sacrificed in case of severe tumor-associated symptoms (i.e., if they were no more able to eat and drink) by an intraperitoneal injection of an overdose of ketamine and xylazine, and perfused with 100 ml of 0.1 mol/l cold PBS (pH 7.4, 4°C). The brains were removed, cut coronally at the injection site, immersed in a cryoprotective medium (Tissue-Tek™, Sakura Finetek, Zoeterwoude, The Netherlands), chilled in liquid nitrogen and stored at -80°C. For histochemical studies, coronal brain sections were made at 10-µm intervals.

Histology and Immunohistochemistry

The gross morphology of the tumors was estimated after staining the coronal brain sections with hematoxylin and eosin (H&E). Immunohistochemical staining was performed with mouse-anti-rat monoclonal antibodies directed against CD45 (diluted 1/500), CD8a (1/600), and CD4 (diluted 1/100; both from Becton-Dickinson, Heidelberg, Germany), ED1 (1/500; Acris, Hiddenhausen, Germany), and CD11b (1/800; Serotec, Düsseldorf, Germany). Subsequently tissues were reacted with the secondary biotinylated rat-absorbed horse-anti-mouse antibodies, followed by avidin/biotinyl-peroxidase complexes (Vector Laboratories, Burlingame, CA, USA). Next, a diaminobenzidine-glucose oxidase technique was applied for immunoperoxidase labeling. Finally, sections were counterstained with hematoxylin. Omission of primary antibodies in control experiments resulted in the expected absence of any cellular labeling.

Data analysis

Descriptive results of tumor volumes in the 9L- and the 9L+HISE groups were presented as box plots using median, minimum, maximum, and both quartiles. Statistical differences between the groups were determined by the Wilcoxon rank sum test, and a P value $< .05$ was considered statistically significant. Survival times of the animals in both groups were obtained by Kaplan-Meier-estimates, and differences between survival curves were calculated using the Log-rank test, considering again $P< .05$ statistically significant. Statistical analysis was performed using SPSS 17 software.

Results

HISE-mediated oncolysis was ineffective in vitro

Incubation of 10^5/ml 9L cells in DMEM with or without concomitant incubation with 10^5/ml HISE particles resulted in a tenfold increase in cell number after 7 days to 10^6/ml in either case. Even by adding $6x10^7$/ml HISE particles, although outnumbering the HISE to 9L-ratio of 1:1 used in the animal experiments by 100x, gliosarcoma cells had tripled in number after 7 days. Therefore, *in vitro*-toxicity of HISE as used for the i.c. injection could be ruled out.

Heat-inactivated staphylococci delayed tumor growth and prolonged survival

All animals tolerated the surgical procedure well, without postoperative neurological abnormalities, weight loss or infectious complications. Stereotactic implantation of 10^5 9L cells in 25µl PBS into the right striatum resulted in gliosarcoma formation in all (n=6) Wistar rats at the site of the implantation, whereas in only 9 of 12 animals receiving additional 10^5 HISE particles an intracerebral tumor could be confirmed by MRI.

Survival times differed markedly between both groups. Animals in the 9L-group died after a mean time of 17.8 d [median 18 d, range15-20 d]. In the HISE-treated group, 8 out of 9 animals that had developed gliosarcomas also died of the tumor burden, but showed a significant increase in average survival to 24.1 d [median 23 d, range 19-35 d] (Fig. 1). However, in one animal of the HISE-group, MRI demonstrated the formation of a mass within the right striatum, but after having reached its peak volume at day 19 it gradually regressed completely (Fig. 5A).

Tumor volumes in both groups could be statistically compared exclusively at day 13, since 5 out of 6 rats in the 9L-group had already died at the time of the follow-up MRI examination at day 19. Tumor growth was delayed in the HISE-treated rats, which

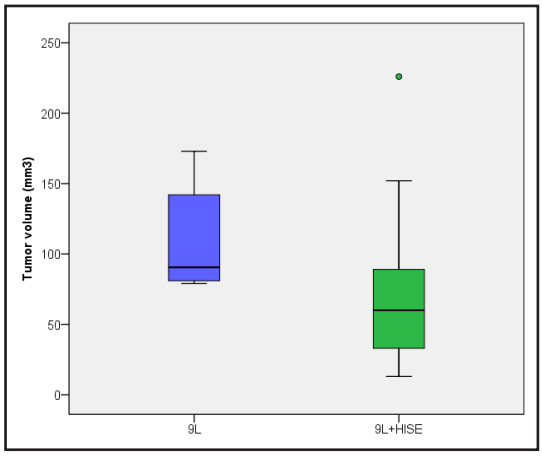

Fig. 1. Kaplan-Meier estimate showing prolonged survival time of 9L gliosarcoma bearing experimental animals after synchronous inoculation of heat-inactivated *S. epidermidis* (HISE) (n=9) in contrast to control animals (n=6) (P < .001, log-rank-test).

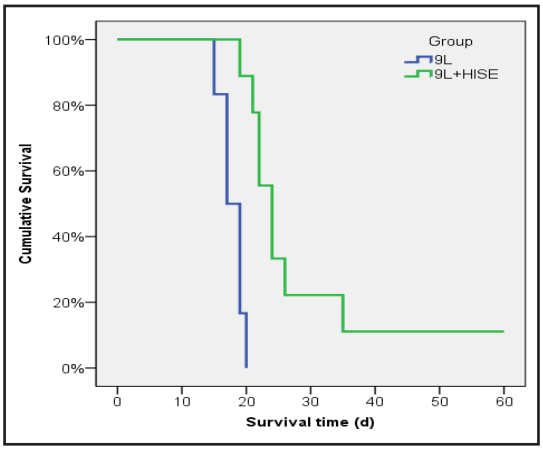

Fig. 2. Box plots comparing tumor volumes of naïve 9L gliosarcoma and after concomitant HISE treatment at 13 days. Although median values in the HISE-treated animals were lower than those in controls, the difference was not significant between both groups (P = .145, Wilcoxon-test).

demonstrated a median mass volume of 60 µl (average: 77.8 µl) at day 13, in comparison to 90.5 µl (average: 109.3 µl) in untreated animals. However, the growth retardation in the HISE-group was not statistically significant (Fig. 2). At day 19, the median tumor volume in the latter group was 171 µl (average: 184.6 µl), whereas the mass of the remaining animal in the 9L-group was 305 µl. In control animals injected with 25 µl PBS, no intracerebral abnormalities apart from a circumscribed edema or scar formation along the needle track could be demonstrated on MRI (data not shown).

Naïve endogenous cellular immune reaction was inefficient to effectively restrain 9L gliosarcoma growth

Animals exclusively injected with 9L cells developed gliosarcomas appearing on MRI as well demarcated lesions with a distinct and homogeneous gadolinium enhancement (Fig. 3A). Histopathological examination revealed the tumors as round, monomorphic and sharply delineated masses with little invasion into the contiguous brain (Fig. 3B). The tumors were hypercellular and composed of spindle-shaped cells of a sarcomatoid phenotype with pleomorphic nuclei and numerous mitotic figures (Fig. 3C). Immunolabeling revealed an infiltration of scattered ED1$^+$ activated macrophages, most of them localized within the outer regions of the mass, but hardly found in the adjacent brain parenchyma (Fig. 3D). Loosely assembled CD8a$^+$ lymphocytes, mainly representing cytotoxic T-cells, could be observed especially at the tumor border and to a lesser extent within the mass, thus overlapping with the distribution of the activated macrophages (Fig. 3E). On the other hand, CD4$^+$ T-lymphocytes were scattered throughout the whole lesions, in part accumulating in small clusters (Fig. 3F). In 2 of the 6 gliosarcomas of the 9L-group, small necrotic areas were present in the center of the lesions. However, no increase in the cellular immune reaction could be observed within or adjacent to these regions. In the 9L group, the impact of anti-tumor immune response apparently did not exert any significant oncolytic potential, since no tumor regression could be observed despite the presence of ED1$^+$ and CD4$^+$/ CD8a$^+$ cells.

Control animals injected with PBS showed a hardly discernible cellular infiltration directly adjacent to the needle track consisting merely of some loosely arranged ED1$^+$ macrophages (data not shown).

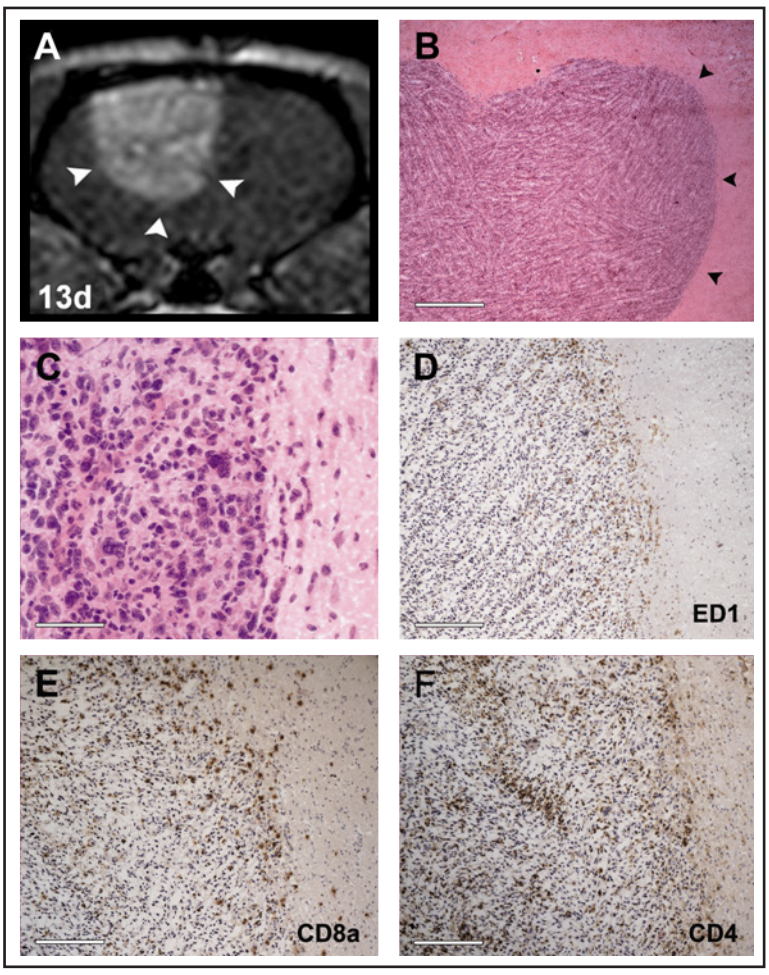

Fig. 3. Morphological and immunological characteristics of intracerebral 9L gliosarcoma in Wistar rats. MRI depicts the tumor as a solid mass (arrowheads) with an intense and almost homogeneous contrast enhancement (A). Representative HE-staining demonstrates a well-delineated lesion (arrowheads) with a compact arrangement (B), consisting of pleomorphic tumor cells with numerous mitotic figures (C). Immunohistological assessment of immune cell response reveals a minor infiltration by ED1$^+$ macrophages and CD8a$^+$ cytotoxic T-lymphocytes, both mainly localized at the outer regions of the tumor but scarcely outside the lesion (D,E), and by scattered CD4$^+$ T-lymphocytes (F). D-F: immunoperoxidase staining dark, HE-counterstaining. Scale bars indicate 500 µm (B), 50 µm (C); and 200 µm (D,E, and F). Original magnification x2.5 (B), x40 (C) and x10 (D,E, and F).

HISE treatment led to a distinct activation of immune response and oncolysis

In HISE-treated animals, MRI showed a clearly reduced contrast enhancement of the lesions in comparison to the 9L-group at 13d in 5 of 9 tumor-bearing animals. At day 19, the pattern of gadolinium uptake of the masses was low in all animals of the HISE-group, either occurring as a homogeneously poor uptake (n=3), as a patchy enhancement (n=2), or as a ringwall enhancement with a central sparing (n=4) (Fig. 4A). HE-staining revealed an extensive oncolysis of the central mass in 4 brains with residual tumor remaining mainly at the periphery (Fig. 4B), and large-scale but less coalescing necrotic regions in the center of the gliosarcomas in another 2 cases. Three tumors showed only minor regressive changes. Hence, a considerable central eradication of the malignancy was observed in two thirds of the HISE-treated animals. At higher magnification, the oncolytic areas showed a mesh-like infiltration of variously shaped mononuclear cells and cellular debris, whereas neutrophilic granulocytes and tumor cells were virtually absent (Fig. 4C). Immunohistochemical staining confirmed an extensive peri- and intratumoral immune response in animals exhibiting central oncolysis. Numerous macrophages surrounded the tumor, distinctly infiltrating the solid portions and forming a dense ribbon around the oncolytic core (Fig. 4D). Moreover, the reticulated matrix within the necrotic center was also extensively interspersed by numerous macrophages (Fig. 4E). Cytotoxic T-lymphocytes were more numerous than macrophages and displayed a different spatial arrangement as they embanked at the outer tumor margins (Fig. 4F). However, they occurred less frequently within the inner solid portions and were

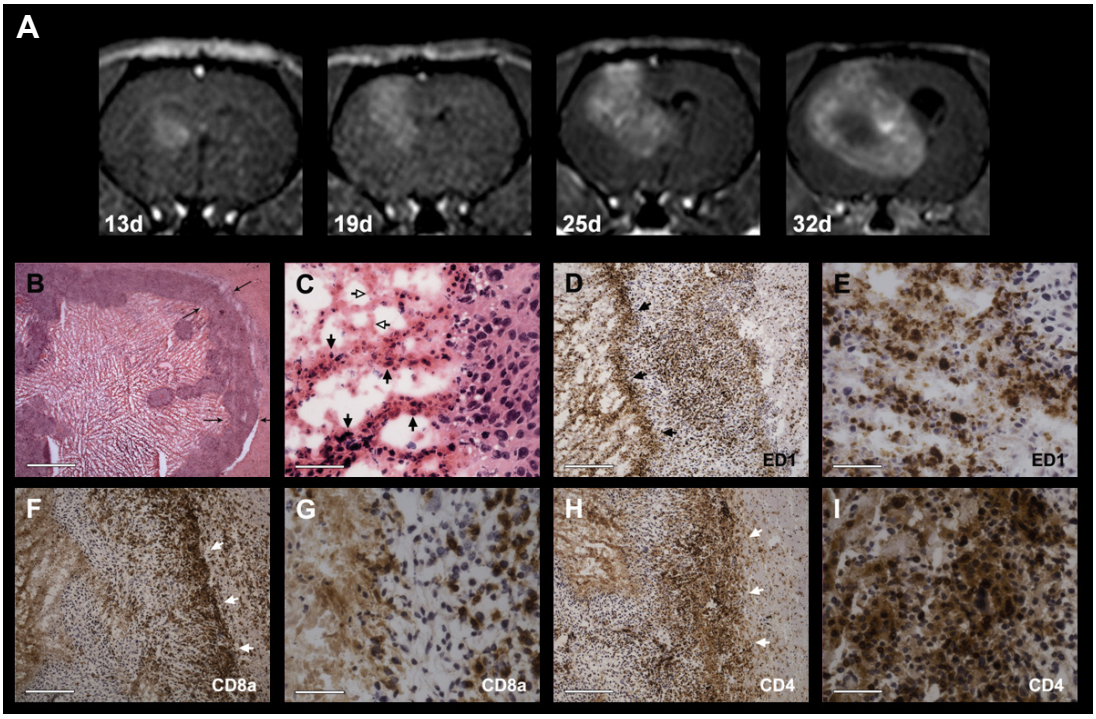

Fig. 4. Effects of HISE on 9L gliosarcoma growth. Serial MRIs from days 13 to 32 show a diminished gadolinium uptake of the early lesions in contrast to the controls, and a central sparing with a ringwall enhancement in the later stages of tumor progress (A). Correspondingly, HE-staining demonstrates a marked regression of the central mass with only small marginated tumor remnants left (arrows) (B). The reticulated matrix inside the lesion consists mainly of different mononuclear cells (closed arrows) intermingled with cellular debris (open arrows), whereas tumor cells are virtually absent in this region (C). Immunohistochemical analysis reveals a marked infiltration of ED1$^+$ macrophages surrounding and infiltrating the marginated tumor, assembling around the oncolytic center like a palisade (arrows) (D), and extensively dissociating the reticulated core of the lesion (E). Infiltration by CD8a$^+$ cytotoxic T-cells is even more pronounced at the outer margins of the residual tumor (arrows) (F), but is almost completely lacking within its necrotic core (G). Moreover, a massive embankment-like infiltration of the peripheral lesion by CD4$^+$ T-lymphocytes (arrows) could be observed (H), that are also disseminated within the central oncolysis (I). D-I: immunoperoxidase staining dark, HE- counterstaining. Scale bars indicate 500 µm (B), 50 µm (C,E,G, and I); and 200 µm (D,F, and H). Original magnification x2.5 (B), x40 (C,E,G, and I) and x10 (D,F, and H).

completely missing in the central oncoloytic region (Fig. 4G). CD4$^+$ T-lymphocytes were crowding in peripheral areas of the gliosarcoma more extensively than cytotoxic T-cells (Fig. 4H), thereby, as macrophages, dissociating the reticulated architecture of the necrotic core (Fig. 4I).

The considerable reinforcement of the cellular immune reaction resulting from HISE treatment led to an extensive oncolysis of the lesions in most animals. In one case it even resulted in a complete regression of the tumor. After rapid growth of the malignancy featuring an inhomogeneous contrast enhancement at day 19, it gradually regressed, accompanied by a decreasing gadolinium uptake, and ultimately resulted in a hypointense porencephalic defect (Fig. 5A). H&E-stained sections of this region disclosed brain tissue with a gliotic border encasing a spongy matrix traversed by large caliber vessels and numerous rounded cells (Fig. 5B), at a higher magnification clearly discernible as ochreous foamy macrophages (Fig. 5C), whereas gliosarcoma cells were absent.

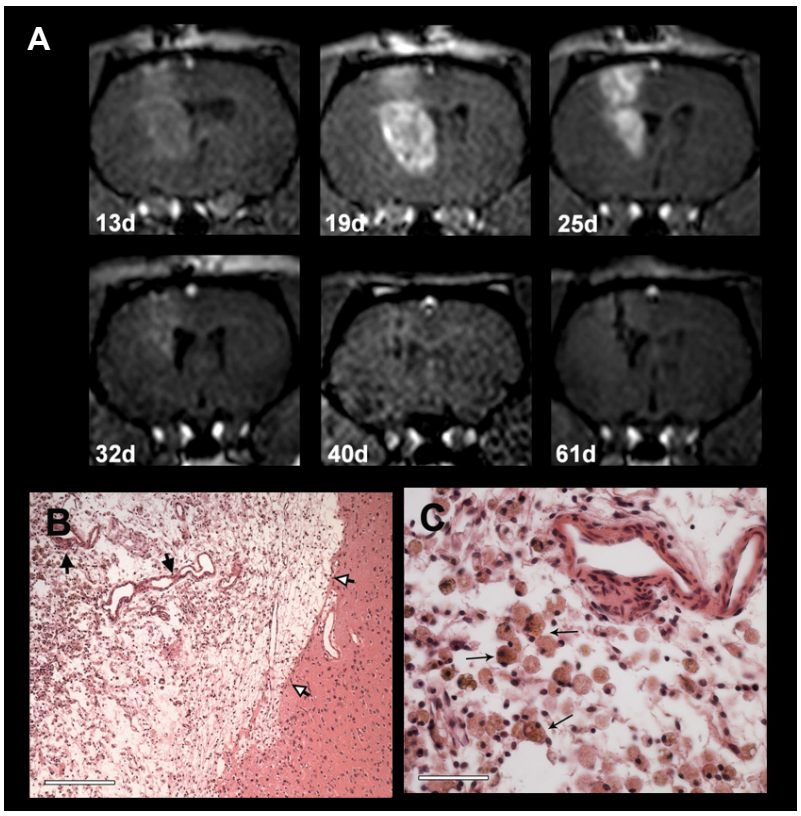

Fig. 5. Complete regression of a 9L gliosarcoma after concomitant HISE treatment. Serial MRI sections clearly demonstrate a progressive increase in tumor size at first, followed by a gradual disappearance of the contrast-enhancing mass lesion and a parenchymal defect in the final state (A). Histological sections after HE-staining demonstrate the defect zone composed of a loosely reticulated, vascularized (closed arrows) tissue surrounded by a gliotic scar (open arrows) (B) and crowded with big foamy macrophages (arrows) (C). Scale bars indicate 200 µm (B); and 50 µm (C). Original magnification x 10 (B) and x40 (C).

Discussion

Our study provides a strong evidence for an immune-mediated antitumor effect of HISE leading to prolonged survival and even cure from experimental 9L gliosarcoma**.** The common mechanism of action of such immunostimulatory adjuvants (ISA) like inactivated whole bacteria such as *S. epidermidis* [19] or *Bacillus Calmette-Guérin* [20], bacterial cell-wall peptides [21-23], or synthetic molecules like imiquimod [24, 25] is the activation of Toll-like receptors, and the subsequent attraction and stimulation of antigen-presenting cells resulting in selective lysis of glioma cells.

Once recruited to the site of the tumor in the 9L animal model, the individual leukocyte populations might inhibit gliosarcoma growth by different mechanisms.

$CD8a^+$ cells, mainly representing cytotoxic T lymphocytes (CTLs) that can directly lyse tumor cells, extensively infiltrated the proliferating parts of the tumor while completely sparing the central necrosis, indicating their attraction by viable malignant cells. Since we demonstrated recently that the widespread infiltration of CTLs after i.c. HISE injection reached its peak on day 4 and fell off thereafter [19], we hypothesize that only the initial steps of the cytotoxic response were triggered by HISE. The sustained trafficking of CTLs was possibly due to their specific targeting of tumor-associated antigens, probably after T-cell priming and clonal expansion in CNS-draining lymph nodes and subsequent homing back to the site of the antigenic threat in the brain [26]. Thus, HISE might act as a potent initiator for an effective homing of tumoricidal CTLs to the 9L gliosarcoma resulting in an extensive oncolysis. In contrast, 9L gliosarcoma without the adjunct of HISE failed to recruit significant numbers of $CD8a^+$ cells to the tumor site. Indeed, effective eradication of malignant glioma is particularly dependent on a powerful CTL response, and a mathematical model demonstrated that several adoptive immunotherapy trials presumably failed because the number of CTLs administered was too small to overcome the immunosuppressive counterattack of the tumor [27].

The massive accumulation of macrophages adjacent to and dissociating the whole gliosarcoma was at least in part induced by HISE, since we could demonstrate macrophages as predominating leukocytes from day 4 on after its i.c. administration [19]. Besides, macrophages were presumably attracted by the necrotic remnants in the center of the lesions, acting there as scavengers like in the animal cured from the gliosarcoma, where they were still detectable in the porencephalic defect. As their putative key function macrophages act as antigen-presenting cells (APCs) to CTLs and provide co-stimulatory signals, triggering proliferation and differentiation of $CD8^+$ T-cells [28]. Moreover, perivascular APCs mediate the migration of $CD4^+$ T- cells across the blood-brain barrier [29] and are mandatory for antigen-specific reactivation of effector T-cells and their persistence within the brain [30], thus illustrating their central role during establishment of a tumor-defensive immune network. However, it remains elusive to what extent these tumor infiltrating macrophages are blood-derived or represent activated microglia, since ED1 stains both and there is no more specific marker.

As was observed with CTLs, the transmigration of $CD4^+$ T- cells into the HISE-treated gliosarcoma is supposed to be initiated by the bacterial epitopes, since naïve tumors showed only minor $CD4^+$ cell infiltration. Their distinct and sustained recruitment is indeed most likely costimulated by tumor-associated antigens, as mere i.c. HISE application resulted in a persistent, but only scattered infiltration as demonstrated recently [19]. To activate a $CD4^+$ response, tumor antigen epitopes must be presented concomitantly with an MHC Class II complex, e.g. on macrophages as APCs. Once activated, $CD4^+$ lymphocytes enhance CTL activation [31] and recruit additional macrophages. On the other hand, an impaired $CD4^+$ T-cell response in the brain would impede $CD8^+$ T-cells from developing into memory cells [32]. Finally, the T-helper (Th) 1 subset of activated $CD4^+$ T-lymphocytes is capable to directly kill malignant cells in several tumors outside the CNS [33], but these direct oncolytic effects are poorly characterized in malignant gliomas.

The extensive immune cell activation and retainment after HISE treatment and the effective antitumor response induced in two thirds of the animals in the HISE-group is likely a two-stage process. Initially, HISE effectively recruits macrophages, CTLs and $CD4^+$ T-cells, as previously demonstrated [19]. Due to absent diffusion capacity and adhesive properties of inactivated staphylococci, the inflammatory reaction keeps confined to the HISE-tumor cell deposit. Afterwards, the already abundantly recruited systemic immune cells cross-react with tumor-associated epitopes, that by itself would be unable to attract a substantial number of T-lymphocytes or macrophages. However, tumor growth has been capable of overcoming the inflammatory attack, since in every fourth case oncolysis and immune cell infiltration was poor despite HISE application. On the other hand, the missing development of a tumor in some HISE-treated animals was presumably caused by an immediate tumoricidal neuroinflammatory response, since toxic effects of HISE *in vitro* could be ruled out.

The 9L gliosarcoma model has been the most extensively used experimental rat brain tumor model [34] and has also been well characterized for its applicability in allogeneic Wistar rats [35]. The 9L cell line was deliberately chosen for the purpose of our experiments for two reasons. First, the 9L gliosarcoma has been shown to secrete the cytokine TGF-beta 2 [36] and in this regard simulate the tumor-induced local immunosuppression of human glioblastoma. Second, 9L cells produce sharply delineated tumors and thereby allow a more reliable morphometrical evaluation by MRI than the utilization of a tumor cell line generating an ill-defined, infiltrative mass [37].

In conclusion, by eradicating the proliferating properties of staphylococci by heat-inactivation, the potential disastrous effects of a postoperative infection could be transformed into a novel immunotherapeutic approach for high-grade glioma. HISE treatment markedly enhanced the number of CTLs, macrophages and $CD4^+$ T-cells at the tumor site and reduced brain tumor growth. Our promising results demonstrate for the first time that inactivated bacteria may be utilized as potent immunostimulatory adjuvants in intracranial tumor therapy. Given the great diversity of bacteria and their different immunomodulatory

properties, our findings might stimulate further investigations to explore their therapeutic potential in the treatment of high-grade glioma.

Acknowledgements

This publication was funded by the German Research Foundation (DFG) and the University of Wuerzburg in the funding programme Open Acces Publishing.

References

1 Stupp R, Hegi ME, Mason WP, van den Bent MJ, Taphoorn MJ, Janzer RC, Ludwin SK, Allgeier A, Fisher B, Belanger K, Hau P, Brandes AA, Gijtenbeek J, Marosi C, Vecht CJ, Mokhtari K, Wesseling P, Villa S, Eisenhauer E, Gorlia T, Weller M, Lacombe D, Cairncross JG, Mirimanoff RO: Effects of radiotherapy with concomitant and adjuvant temozolomide versus radiotherapy alone on survival in glioblastoma in a randomised phase III study: 5-year analysis of the EORTC-NCIC trial. Lancet Oncol 2009;10:459-466.

2 Ge L, Hoa N, Bota DA, Natividad J, Howat A, Jadus M: Immunotherapy of brain cancers: the past, the present, and future directions. Clin Dev Immunol Epub 2011;2010:296453.

3 Nagasawa DT, Fong C, Yew A, Spasic M, Garcia HM, Kruse CA, Yang I: Passive immunotherapeutic strategies for the treatment of malignant gliomas. Neurosurg Clin N Am 2012;23:481-495.

4 Thomas AA, Ernstoff MS, Fadul CE: Immunotherapy for the treatment of glioblastoma. Cancer J 2012;18:59-68.

5 Weller M, Fontana A: The failure of current immunotherapy for malignant glioma. Tumor-derived TGF-ß, T-cell apoptosis, and the immune privilege of the brain. Brain Res Rev 1995;21:128-151.

6 Hishii M, Nitta T, Ishida H, Ebato M, Kurosu A, Yagita H, Sato K, Okumura K: Human glioma-derived interleukin-10 inhibits antitumor immune responses in vitro. Neurosurgery 1995;37:1160-1166;discussion 1166-1167.

7 Zagzag D, Salnikow K, Chiriboga L, Yee H, Lan L, Ali MA, Garcia R, Demaria S, Newcomb EW: Downregulation of major histocompatibility complex antigens in invading glioma cells: stealth invasion of the brain. Lab Invest 2005;85:328-341.

8 Saas P, Walker PR, Hahne M, Quiquerez AL, Schnuriger V, Perrin G, French L, Van Meir EG, de Tribolet N, Tschopp J, Dietrich PY: Fas ligand expression by astrocytoma in vivo: maintaining immune privilege in the brain? J Clin Invest 1997;99:1173-1178.

9 Grauer OM, Wesseling P, Adema GJ: Immunotherapy of diffuse gliomas: biological background, current status and future developments. Brain Pathol 2009;19:674-693.

10 Finocchiaro G, Pellegatta S: Immunotherapy for glioma: getting closer to the clinical arena? Curr Opin Neurol 2011;24:641-647.

11 Bowles AP Jr, Perkins E: Long-term remission of malignant brain tumors after intracranial infection: a report of four cases. Neurosurgery 1999;44:636-643.

12 Kapp JP: Microorganisms as antineoplastic agents in CNS tumors. Arch Neurol 1983;40:637-642.

13 Margolis J, West D: Spontaneous regression of malignant disease: report of three cases. J Am Geriatr Soc 1967;15:251-253.

14 Naganuma H, Sasaki A, Satoh E, Nagasaka M, Isoe S, Nakano S, Nukui H: Long-term survival in a young patient with anaplastic glioma. Brain Tumor Pathol 1997;14:71-74.

15 Walker DG, Pamphlett R: Prolonged survival and pulmonary metastases after local cure of glioblastoma multiforme. J Clin Neurosci 1999;6:67-68.

16 De Bonis P, Albanese A, Lofrese G, de Waure C, Mangiola A, Pettorini BL, Pompucci A, Balducci M, Fiorentino A, Lauriola L, Anile C, Maira G: Postoperative infection may influence survival in patients with glioblastoma: simply a myth? Neurosurgery 2011;69:864-869.

17 Bohman LE, Gallardo J, Hankinson TC, Waziri AE, Mandigo CE, McKhann GM 2nd, Sisti MB, Canoll P, Bruce JN: The survival impact of postoperative infection in patients with glioblastoma multiforme. Neurosurgery 2009;64:828-835.

18 Heppner F, Möse JR: The liquefication (oncolysis) of malignant glioma by a non pathogenic clostridium. Acta Neurochir (Wien) 1978;42:123-125.
19 Löhr M, Molcanyi M, Stenzel W, Seifert H, Tzouras G, Röhn G, Mohseni D, Hampl JA: A novel experimental in vivo model of cerebral immunomodulation induced by inactivated Staphylococcus epidermidis. J Neurosci Methods 2012;203:89-95.
20 Albright L, Seab JA, Ommaya AK: Intracerebral delayed hypersensitivity reactions in glioblastoma multiforme patients. Cancer 1977;39:1331-1336.
21 Eggers AE, Tarmin L: In vitro immunization against autologous glioblastoma cells coupled to adjuvant peptide. J Neurol Sci 1984;63:147-151.
22 Kirsch M, Fischer H, Schackert G: Activated monocytes kill malignant brain tumor cells in vitro. J Neurooncol 1994;20:35-45.
23 Parsa AT, Miller JI, Eggers AE, Ogden AT, Anderson RC: Autologous adjuvant linked fibroblasts induce anti-glioma immunity: implications for development of a glioma vaccine. J Neurooncol 2003;64:77-87.
24 Xiong Z, Ohlfest JR: Topical imiquimod has therapeutic and immunomodulatory effects against intracranial tumors. J Immunother 2011;34:264-269.
25 Prins RM, Soto H, Konkankit V, Odesa SK, Eskin A, Yong WH, Nelson SF, Liau LM: Gene expression profile correlates with T-cell infiltration and relative survival in glioblastoma patients vaccinated with dendritic cell immunotherapy. Clin Cancer Res 2010;17:1603-1615.
26 Calzascia T, Masson F, di Berardino-Besson W, Contassot E, Wilmotte R, Aurrand-Lions M, Rüegg C, Dietrich PY, Walker PR: Homing phenotypes of tumor-specific CD8 T cells are predetermined at the tumor site by crosspresenting APCs. Immunity 2005;22:175-184.
27 Kronik N, Kogan Y, Vainstein V, Agur Z: Improving alloreactive CTL immunotherapy for malignant gliomas using a simulation model of their interactive dynamics. Cancer Immunol Immunother 2008;57:425-439.
28 Calzascia T, di Berardino-Besson W, Wilmotte R, Masson F, de Tribolet N, Dietrich PY, Walker PR: Cutting edge: cross-presentation as a mechanism for efficient recruitment of tumor-specific CTL to the brain. J Immunol 2003:171:2817-2191.
29 Tran EH, Hoekstra K, Van Rooijen N, Dijkstra CD, Owens T: Immune invasion of the central nervous system parenchyma and experimental allergic encephalomyelitis, but not leukocyte extravasation from blood, are prevented in macrophage-depleted mice. J Immunol 1998;161:3767-3775.
30 Masson F, Calzascia T, di Berardino-Besson W, de Tribolet N, Dietrich PY, Walker PR: Brain microenvironment promotes the final functional maturation of tumor-specific effector CD8+ T cells. J Immunol 2007;179:845-853.
31 Stohlman SA, Bergmann CC, Lin MT, Cua DJ, Hinton DR: CTL effector function within the central nervous system requires CD4+ T cells. J Immunol 1998;160:2896-2904.
32 Bevan MJ: Helping the CD8(+) T-cell response. Nat Rev Immunol 2004;4:595-602.
33 Knutson KL, Disis ML: Tumor antigen-specific T helper cells in cancer immunity and immunotherapy. Cancer Immunol Immunother 2005;54:721-728.
34 Barth RF, Kaur B: Rat brain tumor models in experimental neuro-oncology: the C6, 9L, T9, RG2, F98, BT4C, RT-2 and CNS-1 gliomas. J Neurooncol 2009;94:299-312.
35 Stojilkovic M, Piperski V, Dacevic M, Rakic L, Ruzdijc S, Kanazir S: Characterization of 9L glioma model of the Wistar rat. J Neurooncol 2003;63:1-7.
36 Liu Y, Ng KY, Lillehei KO: Time course analysis and modulating effects of established brain tumor on active-specific immunotherapy. Neurosurg Focus 2000;9;e3.
37 Saini M, Bellinzona M, Meyer F, Cali G, Samii M: Morphometrical characterization of two glioma models in the brain of immunocompetent and immunodeficient rats. J Neurooncol 1999;42:59-67.